Radial Flow from Electromagnetic Probes and Signal of Quark Gluon Plasma

Payal Mohanty, Jajati K Nayak, Jan-e Alam and Santosh K Das
Variable Energy Cyclotron Centre, 1/AF, Bidhan Nagar, Kolkata - 700064, INDIA

An attempt has been made to extract the evolution of radial flow from the analysis of the experimental data on electromagnetic probes measured at SPS and RHIC energies. The transverse momentum (p_T) spectra of photons and dileptons measured by WA98 and NA60 collaborations respectively at the CERN-SPS and the photon and dilepton spectra obtained by PHENIX collaboration at BNL-RHIC have been used to constrain the theoretical models. We use the ratio of photon to dilepton spectra to extract the flow, where some model dependence are canceled out. Within the ambit of the present analysis we argue that the variation of the radial velocity with invariant mass is indicative of a phase transition from initially produced partons to hadrons at SPS and RHIC energies.

PACS numbers: 25.75.-q,25.75.Dw,24.85.+p

I. INTRODUCTION

The hot and dense matter expected to be formed in the partonic phase after ultra-relativistic heavy ion collisions dynamically evolve in space and time due to high internal pressure. Consequently the system cools and reverts back to hadronic matter from the partonic phase. Just after the formation, the entire energy of the system is thermal in nature and with progress of time some part of the thermal energy gets converted to the collective (flow) energy. In other words, during the expansion stage the total energy of the system is shared by the thermal as well as the collective degrees of freedom. The evolution of the collectivity within the system is sensitive to the Equation of State (EoS). Therefore, the study of the collectivity in the system formed in the quark gluon plasma (QGP) phase will be useful to shed light on the EoS [1–3] (see [4, 5] for review) and on the nature of the transition that may take place during the evolution process. It is well known that the average magnitude of radial flow at the freeze-out surface can be extracted from the transverse momentum (p_T) spectra of the hadrons. However, hadrons being strongly interacting objects can bring the information of the state of the system when it is too dilute to support collectivity *i.e.* the parameters of collectivity extracted from the hadronic spectra are limited to the evolution stage where the collectivity ceases to exist. These collective parameters have hardly any information about the interior of the matter. On the other hand electromagnetic (EM) probes, *i.e.* photons and dileptons are produced and emitted [6–8] (see [9–11] for review) from each space time points. Therefore, estimating radial flow from the EM probes will shed light on the time evolution of the collectivity in the system [12].

The invariant momentum distribution of photons produced from a thermal source depends on the temperature (T) of the source through the thermal phase space distributions of the participants of the reaction that produces the photon [13]. As a result the p_T spectra of photon reflects the temperature of the source. Hence ideally the photons with intermediate p_T values ($\sim 2-3$ GeV, depending on the value of initial temperature) reflect the properties of QGP (realized when $T > T_c$, T_c is the transition temperature). Therefore, one should look into the p_T spectra for these values of p_T for the detection of QGP. However, for an expanding system the situation is far more complex. The thermal phase space factor changes - several factors *e.g.* the transverse kick received by low p_T photons due to flow originating from the low temperature hadronic phase (realized when $T < T_c$) populates the high p_T part of the spectra [14]. As a consequence the intermediate or the high p_T part of the spectra contains contributions from both QGP and hadrons. For dilepton the situation is, however, different because in this case we have two kinematic variables - out of these two, the p_T spectra is affected by the flow, however, the p_T integrated invariant mass (M) spectra is unaltered by the flow in the system. It should be mentioned here that for M below ρ peak and above ϕ peak dileptons from QGP dominates over its hadronic counterpart (assuming the contributions from hadronic cocktails are subtracted out) within the framework of the present model. However, the spectral function of low mass vector mesons (mainly ρ) may shift toward lower invariant mass region due to non-zero temperature and density effects. As a consequence the contributions from the decays of such vector mesons to lepton pairs could populate the low M window and may dominate over the contributions from the QGP phase [15] (and also [10, 11] for review). In the present work such thermal effects are not considered. All these suggests that a judicious choice of p_T and M windows will be very useful to characterize the flow in QGP and hadronic phase. However, there are still some difficulties. The calculations of EM probes from thermal sources depend on the parameters like initial temperature (T_i), ther-

malization time (τ_i), chemical freeze-out temperature (T_{ch}), kinetic freeze-out temperature (T_f) etc, which are not known uniquely. To minimize the dependence of thermal sources on these parameters the importance of the ratio of the transverse momentum spectra of photon to dilepton has been emphasized previously [16–18] in order to overcome the above mentioned uncertainties. It may be mentioned here that in the limit of $M \to 0$ the lepton pairs (virtual photons) emerge as real photons. Therefore, the evaluation of the ratio of the p_T spectra of photons to dileptons for various invariant mass bins along with a judicious choice of the p_T and M windows will be very useful to extract the properties of QGP as well as that of hadronic phase. This will be demonstrated in the present work by analyzing WA98 and PHENIX photons and NA60 and PHENIX dilepton spectra.

The paper is organized as follows. In the next section, the production of thermal photons and dileptons are briefly outlined. In section III the expansion dynamics of the system is discussed. Section IV is devoted to results and discussions and finally in section V, we present summary and conclusions.

II. PHOTONS AND DILEPTONS PRODUCTION

The p_T and M spectra of EM probes measured in the experiments are mingled with all the sources of productions - broadly categorized as: (i) prompt productions resulting from the interactions of the partons of the colliding nuclei, (ii) thermal productions from the interactions of thermal partons as well as from thermal hadrons and (iii) finally from the decays of the long (compared to strong interaction time scale) lived mesons. The contributions from pp collisions at a given collision energy can be used as a bench-mark to estimate the hard contributions. To estimate the thermal contributions we adopt the following procedure: *thermal contributions=contributions from heavy ion collision minus* $N_{coll}\times$*contributions from pp collisions* where N_{coll} is the number of nucleon-nucleon interactions in the nuclear collisions at a given centrality. Instead of evaluating the hard contributions by applying pQCD we use the experimental data both for photons and dileptons from the pp collisions wherever available to minimize the uncertainties in the contributions of category (i).

For collisions with large nuclei *e.g.* $Au + Au$ or $Pb + Pb$, the number of valence d quarks are more than the number of valence u quark because in these nuclei there are more neutrons than protons. The magnitude of electric charge of the d quark is half of that of u quarks. Consequently, in the production of EM probes from $Au + Au$ collisions - a larger number d quarks with lesser charge and comparatively a smaller number of u quarks with larger charge are involved. Therefore, for the photon production from $Au + Au$ interaction for the category (i) is not a mere superposition of the yield from $p + p$ interaction. However, in the present work we concentrate in the kinematic region of central rapidity where the number of valence quarks are small. In fact, this is negligible for RHIC energy. It is worth mentioning here that the role of EM probes produced from other mechanisms - like fragmentation of high energy quarks and the interaction of high energy partons with thermal QGP medium [19] are ignored here. It is expected that at the p_T domain of our interest omission of these mechanism will not change the final results significantly.

A. Production of thermal photons and dileptons

For the present work photons and dileptons from thermalized matter of partons and hadrons play the most crucial role. The rate of thermal dilepton production per unit space-time volume per unit four momentum volume is given by [6–9]

$$\frac{dR}{d^4p} = \frac{\alpha}{12\pi^4 p^2} L(p^2) \mathrm{Im}\Pi^{R\mu}_{\mu} f_{BE} \qquad (1)$$

where α is the EM coupling constant, $\mathrm{Im}\Pi^{\mu}_{\mu}$ is the imaginary part of the retarded photon self energy and $f_{BE}(E,T)$ is the thermal phase space distribution for Bosons. $L(p^2)=(1+2m^2/p^2)\sqrt{1-4m^2/p^2}$, arises from the final state leptonic current involving Dirac spinors of mass m. As mentioned before, in the limit of vanishing M a lepton pair *i.e.* a virtual photon appears as a real photon. Therefore, the real photon production rate can be obtained from the dilepton emission rate by replacing the product of EM vertex $\gamma^\star \to l^+l^-$, the term involving final state leptonic current and the square of the (virtual) photon propagator by the polarization sum for the real photon. For an expanding system E should be replaced by $u_\mu p^\mu$, where p^μ and u^μ are the four momentum and the hydrodynamic four velocity respectively.

B. Thermal photons

The Hard Thermal Loop [20] approximations has been used by several authors [21] to evaluate the photon spectra originating from a thermal source of quarks and gluons. The complete calculation of emission rate of photons from QGP to order $\mathrm{O}(\alpha\alpha_s)$ has been done by resuming ladder diagrams in the

effective theory [22], which has been used in the present work. A set of hadronic reactions with all possible isospin combinations have been considered for the production of photons [23–25] from hadronic matter. The effect of hadronic dipole form factors has been taken into account in the present work as in [25].

C. Thermal dileptons

The lowest order process producing lepton pairs is q and $\bar{q}$ annihilation. The correction of order $\alpha_s\alpha^2$ to the lowest order rate of dilepton production from QGP has been calculated in [26, 27], which is considered in the present work. For the low M dilepton production from the hadronic phase the decays of the light vector mesons ρ, ω and ϕ has been considered in [10, 11, 28]. The continuum part of the vector mesons spectral functions constrained by experimental data [28] have been included here. As mentioned before the contributions from the QGP phase dominates the M spectra of the lepton pairs below ρ-peak and above the ϕ-peak if no thermal effects of the spectral functions of the vector mesons (see [10, 11, 29] for review) are considered. Since the continuum part of the vector meson spectral functions are included in the current work the processes like four pions annihilations [30] are excluded to avoid double counting.

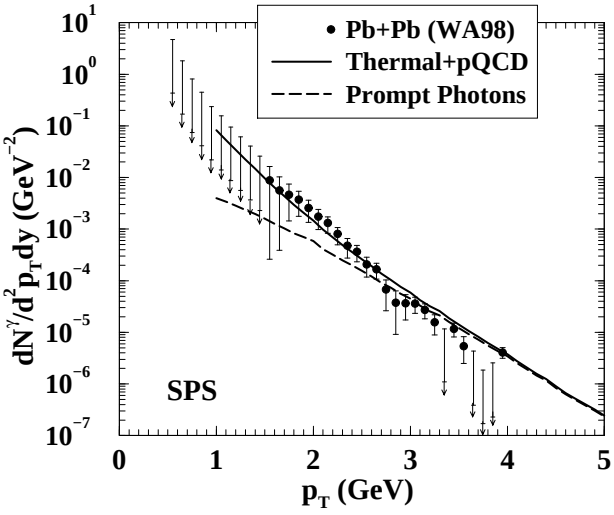

FIG. 1: Transverse momentum spectra of photon at SPS energy for Pb+Pb collision at mid rapidity.

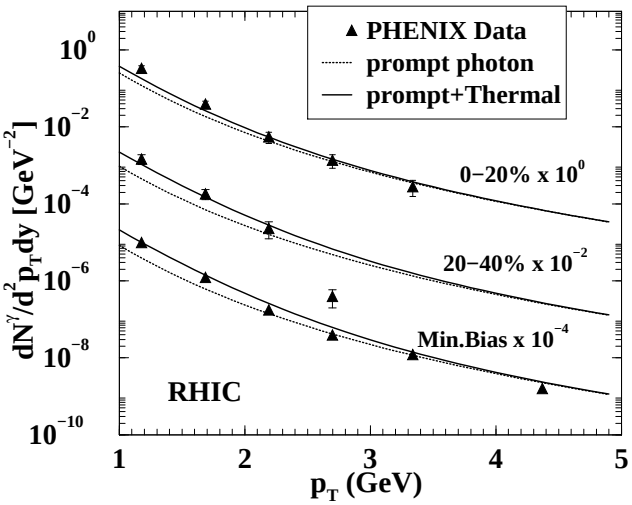

FIG. 2: Transverse momentum spectra of photons at RHIC energy for Au-Au collision for different centralities at mid-rapidity.

III. EXPANSION DYNAMICS

The space time evolution of the system formed in heavy ion collisions has been studied by using relativistic hydrodynamics with longitudinal boost invariance [31] and cylindrical symmetry [32]. We assume that the system reaches equilibration at a time τ_i after the collision. The initial temperature, T_i can be related to the measured hadronic multiplicity (dN/dy) by the following relation:

$$T_i^3\tau_i \approx \frac{2\pi^4}{45\zeta(3)}\frac{1}{4a_{eff}}\frac{1}{\pi R_A^2}\frac{dN}{dy}. \qquad (2)$$

where R_A is the radius of the system, $\zeta(3)$ is the Riemann zeta function and $a_{eff} = \pi^2 g_{eff}/90$ where g_{eff} $(= 2\times 8 + 7\times 2\times 2\times 3\times N_F/8)$ is the degeneracy of quarks and gluons in QGP, N_F=number of flavours. The value of dN/dy for various beam energies and centralities are calculated from the following equation [33]:

$$\frac{dN}{dy} = (1-x)\frac{dn_{pp}}{dy}\frac{< N_{part} >}{2} + x\frac{dn_{pp}}{dy} < N_{coll} > \qquad (3)$$

and tabulated in table I. N_{coll} is the number of collisions and contribute to x fraction to the multiplicity dn_{pp}/dy measured in pp collision. The number of participants, N_{part} contributes fraction $(1-x)$ of dn_{pp}/dy. The values of N_{part} and N_{coll} are estimated by using Glauber Model and the results are in agreement with [34]. We have used $dn_{pp}/dy = 2.43$ and $x = 0.1$ at $\sqrt{s_{NN}} = 200$ GeV. It should be mentioned here that the values of dN/dy

TABLE I: The values of various parameters - thermalization time (τ_i), initial temperature (T_i) and hadronic multiplicity dN/dy - used in the present calculations.

$\sqrt{s_{NN}}$	centrality	$\frac{dN}{dy}$	$\tau_i(fm)$	T_i(MeV)
17.3 GeV	0-06%	700	1.0	200
200 GeV	0-20%	496	0.6	227
	20-40%	226	0.6	203
	min. bias	184	0.6	200

(through N_{part} and N_{coll} in Eq. 3) and hence the T_i (through dN/dy in Eq. 2) depend on the centrality of the collisions. The values of R_A for different centralities have been evaluated by using the equation $R_A \sim 1.1 N_{part}^{1/3}$. Some comments are in order here regarding the flow for non-central collisions which results in non-cylindrical geometrical shape of the system formed after the collisions. In the present work the non-centrality of the nuclear collisions is reflected in the initial temperature through hadronic multiplicity. The geometry of the system due to non-centrality, should in principle be treated by (2+1) dimensional [35] or for more rigorous treatment (3+1) dimensional hydrodynamical [36] evolution. However, we expect that the results obtained in the present work will not be affected substantially due to non-cylindrical geometric shape of the system. Because the flow has been extracted from the ratio of photon to dilepton spectra for a given centrality.

We use the EoS obtained from the lattice QCD calculations by the MILC collaboration [37]. We consider kinetic freeze out temperature, T_f=140 MeV for all the hadrons. The ratios of various hadrons measured experimentally at different $\sqrt{s_{\rm NN}}$ indicate that the system formed in heavy ion collisions chemically decouple at $T_{\rm ch}$ which is higher than T_f which can be determined by the transverse spectra of hadrons [38]. Therefore, the system remains out of chemical equilibrium from $T_{\rm ch}$ to T_f. The deviation of the system from the chemical equilibrium is taken in to account by introducing chemical potential for each hadronic species. The chemical non-equilibration affects the yields through the phase space factors of the hadrons which in turn affects the productions of the EM probes. The value of the chemical potential has been taken in to account following Ref. [3]. It is expected that the chemical potentials do not change much for the inclusion of resonances above Δ.

IV. RESULTS AND DISCUSSION

A. p_T distributions of photons and dileptons

The prompt photons and dileptons (Drell-Yan) are normally estimated by using perturbative QCD. However, to minimize the theoretical model dependence here we use the available experimental data from pp collisions to estimate the hard photon and dilepton contributions in heavy ion collisions. The WA98 photon spectra from Pb+Pb collisions is measured at $\sqrt{s_{NN}}$ = 17.3 GeV. However, no data at this collision energy is available for pp interactions. Therefore, prompt photons for p+p collision at $\sqrt{s_{NN}}$ = 19.4 GeV has been used [39] to estimate the hard contributions for nuclear collisions at $\sqrt{s_{\rm NN}}$ = 17.3 GeV. Appropriate scaling (see [40] for details) has been used to obtain the results at $\sqrt{s_{NN}}$ = 17.3 GeV. For the Pb+Pb collisions the result has been appropriately scaled by the number of collisions at this energy (this is shown in Fig. 1 as prompt photons). The high p_T part of the WA98 data is reproduced by the prompt contributions reasonably well. At low p_T the hard contributions under estimate the data indicating the presence of a thermal source. The thermal photons with initial temperature = 200 MeV along with the prompt contributions explain the WA98 data well (Fig. 1), with the inclusion of non-zero chemical potentials for all hadronic species considered [3](see also [41]). In some of the previous works [42–47] the effect of chemical freeze-out is ignored. As a result either a higher value of T_i or a substantial reduction of hadronic masses in the medium was required [42]. In the present work, the data has been reproduced without any such effects.

Following a similar procedure, the data [48] from Au-Au collisions at $\sqrt{s_{NN}}$ = 200 GeV has been reproduced well by adding the prompt contributions (which is constrained by pp data at the same energy) to the thermal photons. The reproduction of data is satisfactory (Fig. 2) for all the centralities with the initial temperature shown in table I (see also [49].

The transverse mass distribution of dimuons produced in In+In collisions at $\sqrt{s_{NN}}$ = 17.3 GeV has been evaluated for different invariant mass ranges (see [50] for details). The quantity $dN/M_T dM_T$ has been obtained by integrating the production rates over invariant mass windows $M_{\rm min}$ to M_{max} and M_T is defined as $\sqrt{< M >^2 + p_T^2}$ where $< M >= (M_{\rm min} + M_{max})/2$. The results are compared with the data obtained by NA60 collaborations [51] at SPS energy (Fig. 3). Theoretical results contain contributions from the thermal decays of light vector mesons (ρ, ω and ϕ) and also from the decays of vector mesons at the freeze-out [52] of the system has also been considered. The non-monotonic varia-

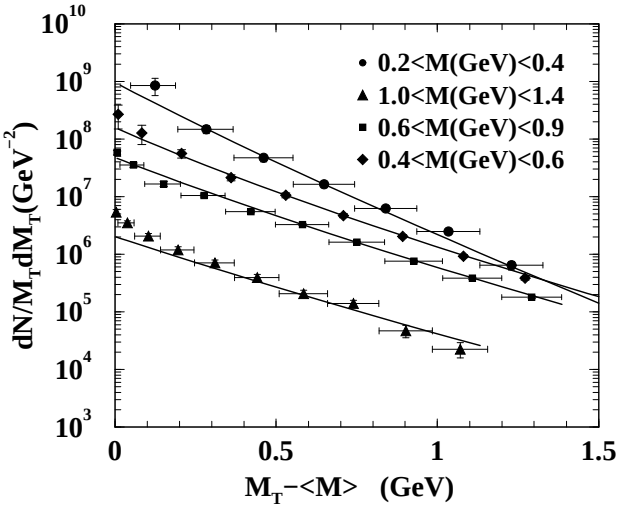

FIG. 3: Transverse mass spectra of dimuons in In+In collisions at SPS energy. Solid lines denote the theoretical results.

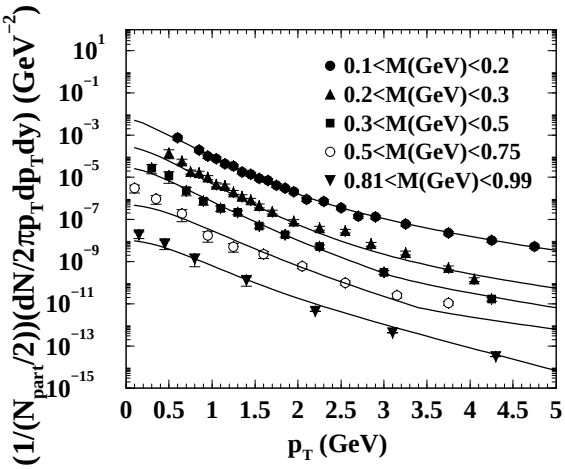

FIG. 4: Transverse momentum spectra of dileptons for different invariant mass windows for minimum bias Au-Au collisions at RHIC energy.

tion of the effective slope parameter extracted from the M_T spectra of the lepton pair with $\langle M \rangle$ evaluated within the ambit of the present model [50] reproduces the NA60 [51] results reasonably well. For Au+Au collisions at $\sqrt{s_{NN}}$=200 GeV, we have evaluated the dilepton spectra for different invariant mass bins with the initial condition (min bias) shown in Table I and lattice QCD equation of state. The results are displayed in Fig. 4. The slopes of the experimental data on p_T distribution of lepton pairs for different invariant mass windows measured by the PHENIX collaboration [53] could be reproduced well with the same initial condition that reproduces photon spectra [48]. In fact, the reproduction of data for the higher mass windows 0.5 <M(GeV)< 0.75 and 0.81 <M(GeV)< 0.99 do not need any normalization factors (Fig. 4). For lower mass windows slopes are reproduced well but fail to reproduce the absolute normalization. Therefore, it should be clarified here that the theoretical results shown in Fig. 4 for lower mass windows (to be precise for 0.1 <M(GeV)< 0.2, 0.2 <M(GeV)< 0.3 and 0.3 <M(GeV)< 0.5) contain arbitrary normalization constant. However, it should also be mentioned at this point that for the extraction of the flow within the present approach the absolute normalization is not essential, which is essential is the slope (Eq. 5). Therefore, the non-reproduction of the absolute normalization of the p_T spectra of lepton pairs for the lower mass windows does not affect the extraction of the magnitude of the radial flow.

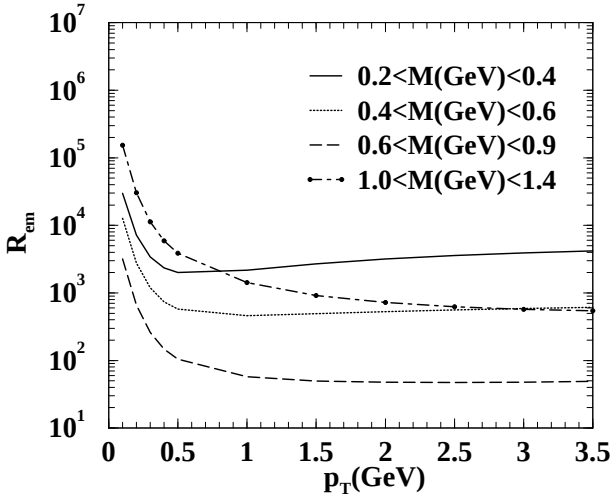

FIG. 5: Variation thermal photon to dilepton ratio, R_{em} with p_T for different invariant mass windows at SPS energy (see text).

B. The ratio, R_{em}

As mentioned before some of the uncertainties prevailing in the individual spectra may be removed by taking the ratio, R_{em} of the p_T distribution of thermal photon to dileptons. In the absence of experimental data for both photon and dilepton from the same colliding system for SPS energies, we have calculated the ratio R_{em} for Pb+Pb system, where the initial condition, the freeze-out condition and the EoS are constrained by the measured WA98 photon spectra. The results are displayed in Fig. 5.

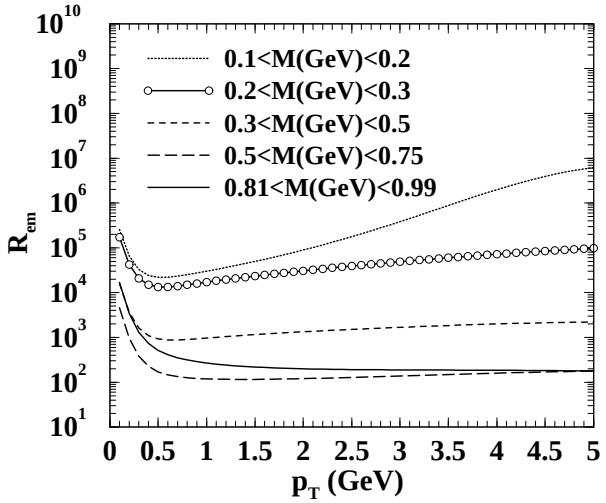

FIG. 6: Variation thermal photon to dilepton ratio, R_{em} with p_T for different invariant mass windows at RHIC energy (see text).

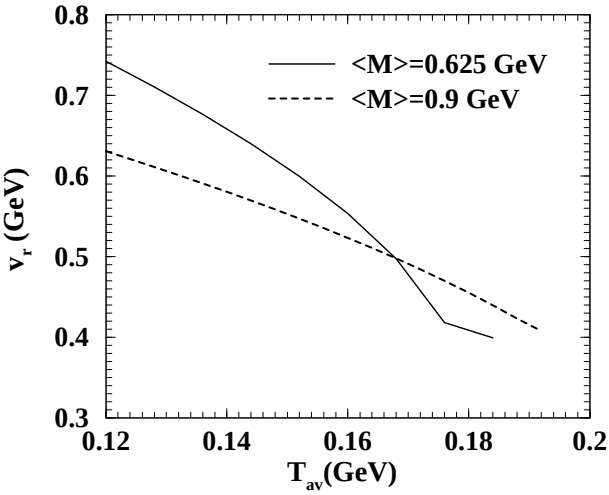

FIG. 8: The variation of radial flow velocity with average temperature of the system for$< M >$ =0.625 GeV and 0.9 GeV at RHIC energy.

Next we evaluate the ratio of the thermal photon to dilepton spectra constrained by the experimental data from Au+Au collisions measured by PHENIX collaboration. The results for the thermal ratio, R_{em} displayed in Fig. 6 is constrained by the experimental data. The behaviour of R_{em} with p_T for different invariant mass windows which is extracted from the available data is similar to the theoretical results obtained in Ref. [17]. The ratio, R_{em} for different M

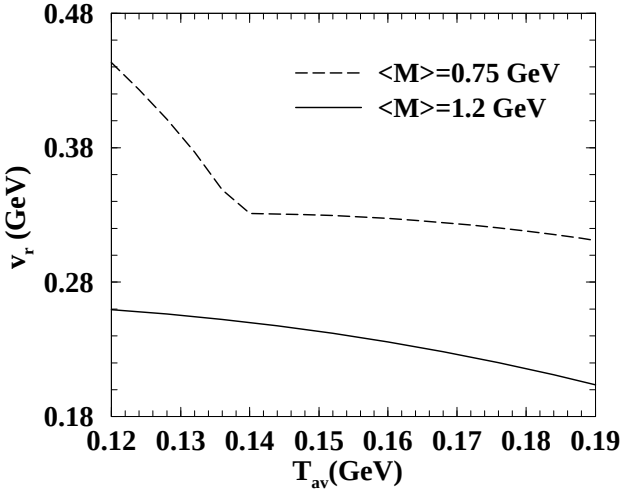

FIG. 7: The variation of radial flow velocity with average temperature of the system for$< M >= 0.75$ GeV and 1.2 GeV at SPS energy.

windows (Figs. 5 and 6) can be parametrized as follows:

$$R_{em} = A\left(\frac{M_T}{p_T}\right)^B \exp\left(\frac{M_T - p_T}{T_{eff}}\right) \qquad (4)$$

with different values of T_{eff} for different invariant mass windows. The argument of the exponential in Eq. 4 can be written as [18];

$$\begin{aligned}\frac{M_T - p_T}{T_{eff}} &= \frac{M_T}{T_{eff2}} - \frac{p_T}{T_{eff1}} \\ &= \frac{M_T}{T_{av} + Mv_r^2} - \frac{p_T}{T_{av}\sqrt{\frac{1+v_r}{1-v_r}}} \end{aligned} \qquad (5)$$

where, $T_{eff1} = T_{av}\sqrt{\frac{1+v_r}{1-v_r}}$ is the blue shifted effective temperature for massless photons and $T_{eff2} = T_{av} + Mv_r^2$, is the effective temperature for massive dileptons. T_{av} is the average temperature and v_r is the average radial flow of the system. For a given p_T and M Eq. 5 can be written as $v_r = f(T_{av})$. The T_{eff} obtained from the parametrization of ratio at SPS energy are 263 MeV and 243 MeV for M=0.75 and 1.2 GeV respectively. The average flow velocity v_r versus T_{av} have been displayed for M=0.75 GeV and 1.2 GeV in Fig. 7. The hadronic matter (QGP) dominates the $M \sim 0.75(1.2)$ GeV region. Therefore, these two mass windows are selected to extract the flow parameters for the respective phases. The v_r increases with decreasing T_{av} (increase in time) and reaches its maximum when the temperature of the system is minimum, i.e., when the system attains T_f, the freeze-out temperature. Therefore, the variation of v_r with T_{av} may be treated as to show

how the flow develops in the system. The v_r is larger in the hadronic phase because the velocity of sound in this phase is smaller, which makes the expansion slower as a consequence system lives longer - allowing the flow to fully develop. On the other hand, v_r is smaller in the QGP phase because it has smaller life time where the flow is only partially developed. In Fig. 8 the variation of average transverse velocity with average temperature for RHIC initial conditions is depicted. The magnitude of the flow is larger in case of RHIC than SPS because of the higher initial pressure. Because of the larger initial pressure and QGP life time the radial velocity for QGP at RHIC is larger compared to SPS.

Obtaining T_{eff1} and T_{eff2} from the individual spectra and eliminating T_{av} one gets the variation of v_r with M. Fig. 9 (left panel) shows the variation of v_r with M for SPS conditions. The radial flow velocity increases with invariant mass M up to $M = M_\rho$ then drops. How can we understand this behaviour? From the invariant mass spectra it is well known that the low M (below ρ mass) and high M (above ϕ peak) pairs originate from a partonic source [17]. The collectivity (or flow) does not develop fully in the QGP because of the small life time of this phase. Which means that the radial velocity in QGP will be smaller for both low and high M. Whereas the lepton pairs with mass around ρ-peak mainly originate from a hadronic source (at a late stage of the evolution of system) are largely affected by the flow resulting in higher values of flow velocity. In summary, the value of v_r for M below and above the ρ-peak is small but around the ρ peak is large - with the resulting behaviour displayed in Fig. 9. Similar non-monotonic behaviour is observed in case of elliptic flow of photon as a function of p_T [54]. The variation of v_r with M in RHIC (Fig. 9 right panel) is similar to SPS, though the values of v_r at RHIC is larger than that of SPS as expected due to higher initial pressure.

laborations have been studied. The initial conditions have been constrained to reproduce the measured multiplicity in these collisions. The EoS, the other crucial input to the calculations has been taken from lattice QCD calculations. The deviation of the hadronic phase from chemical equilibrium is taken in to account by introducing non-zero chemical potential for each hadronic species. It is shown that simultaneous measurements of photon and dilepton spectra in heavy ion collisions will enable us to quantify the evolution of the average radial flow velocity

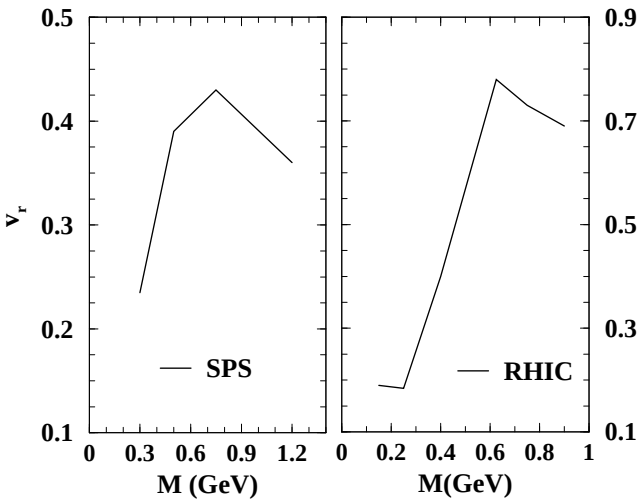

FIG. 9: The variation of radial flow with invariant mass pairs for SPS (left) and RHIC (right) energies.

for the system and the nature of the variation of radial flow with invariant mass indicate the formation of partonic phase at SPS and RHIC energy.

V. SUMMARY AND CONCLUSIONS

The photon and dilepton spectra measured at SPS and RHIC energies by different experimental col-

Acknowledgment: We are grateful to Tetsufumi Hirano for providing us the hadronic chemical potentials. This work is supported by DAE-BRNS project Sanction No. 2005/21/5-BRNS/2455.

[1] E. Schnedermann, J. Sollfrank and U. Heinz, Phys. Rev. C **48** (1993) 2462.
[2] C. M. Hung and E. Shuryak, Phys. Rev. C **57** (1998) 1891.
[3] T. Hirano and K. Tsuda, Phys. Rev. C **66** (2002) 054905.
[4] P. Huovinen and P. V. Ruuskanen, Ann. Rev. Nucl. Part. Sci. **56** (2006) 163.
[5] D. A. Teaney, arXiv:0905.2433 [nucl-th].
[6] L. D. McLerran and T. Toimela, Phys. Rev. D **31** (1985) 545.
[7] C. Gale and J.I. Kapusta, Nucl. Phys. B **357** (1991) 65.
[8] H.A. Weldon, Phys. Rev. D **42** (1990) 2384.
[9] J. Alam, S. Raha and B. Sinha, Phys. Rep. **273** (1996) 243.

[10] J. Alam, S. Sarkar, P. Roy, T. Hatsuda and B. Sinha, Ann. Phys. **286** (2001) 159.

[11] R. Rapp and J. Wambach, Adv. Nucl. Phys. **25** (2000) 1.

[12] T. Renk and J. Ruppert, Phys. Rev. C **77**, 024907 (2008).

[13] C. Y. Wong, Introduction to High Energy Heavy Ion Collisions, World Scientific, Singapore, 1994.

[14] J. Alam, D. K. Srivastava, B. Sinha and D. N. Basu, Phys. Rev. D **48**, 1117 (1993).

[15] J. Ruppert, C. Gale, T. Renk, P. Lichard and J. I. Kapusta, Phys. Rev. Lett. **100**, 162301 (2008).

[16] B. Sinha, Phys. Lett. B **128** (1983) 91.

[17] J. K. Nayak, J. Alam, S. Sarkar and B. Sinha, Phys. Rev. C **78** (2008) 034903.

[18] J. K. Nayak and J. Alam, Phys. Rev. C **80** (2009) 064906.

[19] S. Turbide, C. Gale, E. Frodermann and U. Heinz, Phys. Rev. C **77**, 024909 (2008).

[20] E. Braaten and R. D. Pisarski, Nucl. Phys. B **337** (1990) 569; ibid **339** (1990) 310.

[21] J. Kapusta, P. Lichard, and D. Seibert, Phys. Rev. D **44** (1991) 2774; R. Bair, H. Nakkagawa, A. Niegawa, and K. Redlich, Z. Phys. C **53** (1992)433; P. Aurenche, F. Gelis, R. Kobes, and H. Zaraket, Phys. Rev. D **58** (1998) 085003.

[22] P. Arnold, G.D. Moore, and L.G. Yaffe, J. High Energy Phys. **0111** (2001) 057; P. Arnold, G.D. Moore, and L.G. Yaffe, J. High Energy Phys. **0112** (2001) 009; P. Arnold, G.D. Moore, and L.G. Yaffe, J. High Energy Phys. **0206** (2002) 030.

[23] S. Sarkar, J. Alam, P. Roy , A. K. Dutt-Mazumder, B. Dutta-Roy, B. Sinha, Nucl. Phys. A **634** (1998) 206.

[24] P. Roy, S. Sarkar, J. Alam and B. Sinha, Nucl. Phys. A **653** (1999) 277.

[25] S. Turbide, R. Rapp and C. Gale, Phys. ReV. C **69** (2004) 014903.

[26] T. Altherr and P. V. Ruuskanen, Nucl. Phys. B **380** (1992) 377.

[27] M. H. Thoma and C. T. Traxler, Phys. ReV. D **56** (1997) 198.

[28] E. V. Shuryak, Rev. Mod. Phys. **65** (1993) 1.

[29] G.E. Brown and M. Rho, Phys. Rep. **269** (1996) 333.

[30] P. Lichard and J. Jura, hep-ph/0601234.

[31] J. D. Bjorken, Phys. Rev. D **27** (1983) 140.

[32] H. von Gersdorff, M. Kataja, L. D. McLerran and P. V. Ruskanen, Phys. Rev. D **34** (1986) 794.

[33] D. Kharzeev and M. Nardi, Phys. Lett. B **507** (2001) 121.

[34] S. S. Adler *et al.* (PHENIX collaboration), Phys. Rev. Lett. **91** (2003) 072301.

[35] P. F. Kolb, J. Sollfrank and U. Heinz, Phys. Rev. C **62**, 054909 (2000).

[36] T. Hirano, Phys. Rev. C **65**, 011901 (2002).

[37] C. Bernard *et al.*, Phys. Rev. D **75** (2007) 094505.

[38] I. Arsene *et al.* (BRAHMS Collaboration), Nucl. Phys. A **757** (2005) 1; B. B. Back *et al.* (PHOBOS Collaboration), Nucl. Phys. A **757** (2005) 28; J. Adams *et al.* (STAR Collaboration), Nucl. Phys. A **757** (2005) 102; K. Adcox *et al.* (PHENIX Collaboration), Nucl. Phys. A **757** (2005) 184.

[39] D. L. Adams *et al.*, (E704 Collaboration), Phys. Lett. B **345** (1995) 569.

[40] M.M. Aggarwal *et al.* (WA98 Collaboration), Phys. Rev. Lett. **85** (2000) 3595.

[41] T. Renk, Phys. Rev. C **71**, 064905 (2005; T. Renk, J. Phys. G **30**, 1495 (2004).

[42] J. Alam, S. Sarkar, T. Hatsuda, T. K. Nayak and B. Sinha, Phys. Rev. C **63** (2001) 021901 (R); J. Alam, P. Roy, S. Sarkar and B. Sinha, Phys. Rev. C **67** (2003) 054901.

[43] D. K. Srivastava and B. Sinha, Phys. Rev. C **64**, (2001) 034902.

[44] P. Huovinen, P. V. Ruuskanen and S. S. Rasanen, Phys. Lett. B **535** (2002) 109.

[45] K. Gallmeister, B. Kämpfer and O. P. Pavelenko, Phys. Rev. C **62** (2000) 057901.

[46] F. D. Steffen and M. H. Thoma, Phys. Lett. B **510**, 98 (2001).

[47] R. Chatterjee, D. K. Srivastava and S. Jeon, Phys. Rev. C **79**, 034906 (2009).

[48] A. Adare *et al.* (PHENIX collaboration), arXiv:0804.4168 [nucl-ex].

[49] F.-M. Liu, T. Hirano, K. Werner and Y. Zhu, Phys. Rev. C **79** (2009) 014905.

[50] J. Alam, T. Hirano, J. K. Nayak and B. Sinha, arXiv:0902.0446 [nucl-th]

[51] R. Arnaldi *et al.* for NA60 Collaborations, Phys. Rev. Lett. **100** (2008) 022302.

[52] E. Cooper and G. Frye, Phys. Rev. D **10** (1974) 186.

[53] A. Toia (PHENIX Collaboration), J. Phys. G **35** (2008) 104037, A. Adare *et al.* (PHENIX Collaboration),Phys. Rev. C **81**, 034911 (2010).

[54] F.-M. Liu, T. Hirano, K. Werner and Y. Zhu, arXiv:0906.3566; R. Chatterjee, E. S. Frodermann, U. W. Heinz and D. K. Srivastava, Phys. Rev. Lett. **96** (2006) 202302.

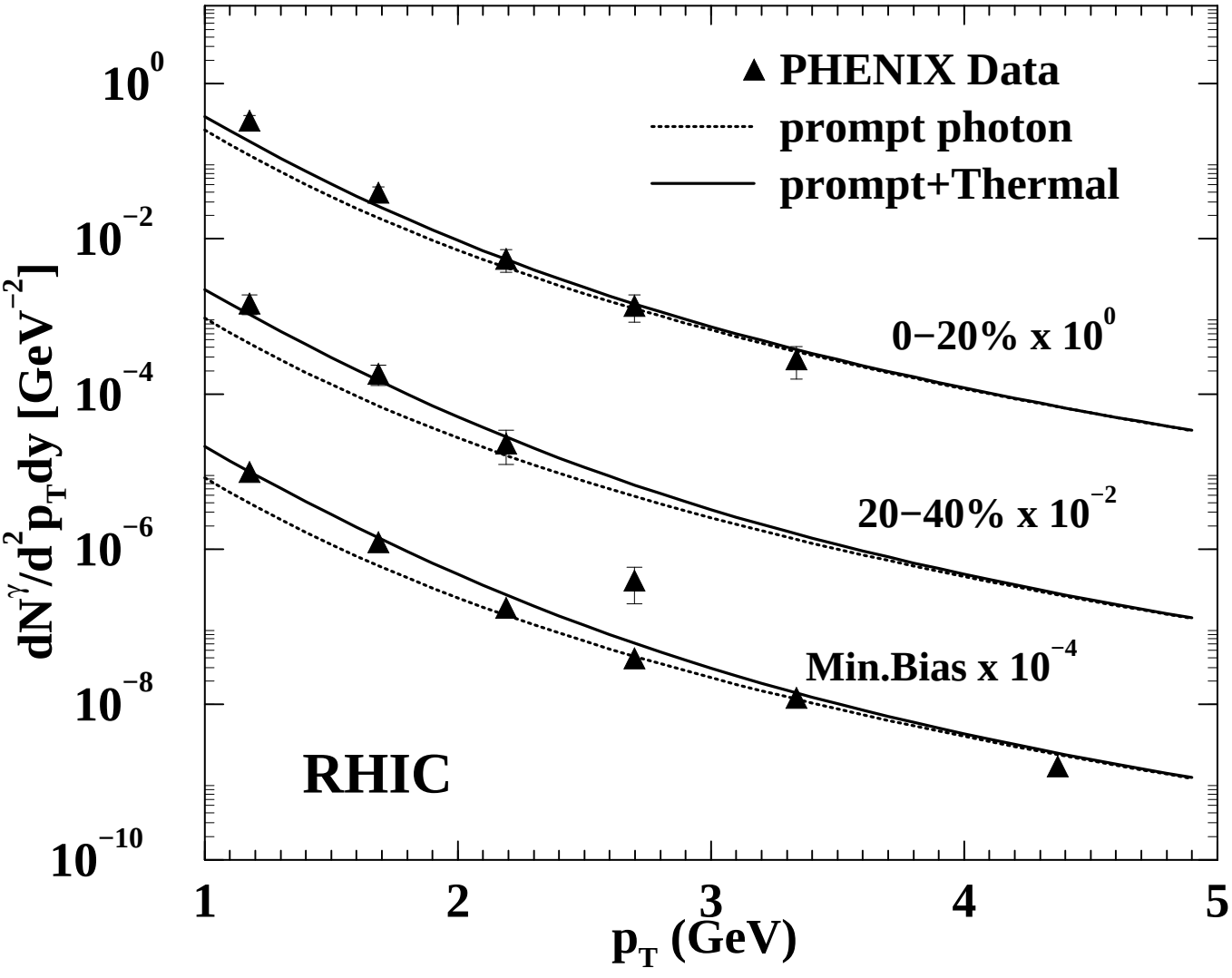
PHENIX Data
prompt photon
prompt+Thermal
0−20% x 10^0
20−40% x 10^−2
Min.Bias x 10^−4
RHIC
dN^γ/d^2p_T dy [GeV^−2]
p_T (GeV)
10^0
10^−2
10^−4
10^−6
10^−8
10^−10
1
2
3
4
5